

Humidity-independent conducting polyaniline films synthesized using advanced atmospheric pressure plasma polymerization with in-situ iodine doping

Choon-Sang Park, Do Yeob Kim, Dong Ha Kim, Hyung-Kun Lee, Bhum Jae Shin, and Heung-Sik Tae

Citation: *Appl. Phys. Lett.* **110**, 033502 (2017); doi: 10.1063/1.4974222

View online: <http://dx.doi.org/10.1063/1.4974222>

View Table of Contents: <http://aip.scitation.org/toc/apl/110/3>

Published by the [American Institute of Physics](#)

Humidity-independent conducting polyaniline films synthesized using advanced atmospheric pressure plasma polymerization with *in-situ* iodine doping

Choon-Sang Park,^{1,a)} Do Yeob Kim,^{2,a)} Dong Ha Kim,¹ Hyung-Kun Lee,² Bhum Jae Shin,³ and Heung-Sik Tae^{1,b)}

¹School of Electronics Engineering, College of IT Engineering, Kyungpook National University, Daegu 702-701, South Korea

²ICT Materials and Components Research Laboratory, Electronics and Telecommunications Research Institute (ETRI), Daejeon 34129, South Korea

³Department of Electronics Engineering, Sejong University, Seoul 143-747, South Korea

(Received 1 November 2016; accepted 5 January 2017; published online 18 January 2017)

This study reports on the synthesis and characterization of conducting polyaniline (PANI) thin films when using advanced atmospheric pressure plasma jets (APPJs). A simple method for synthesizing conducting polymers (CPs) with humidity-independent characteristics is introduced using advanced APPJs and an *in-situ* iodine doping method. In the case of *ex-situ* I₂ doping, a humidity effect study showed that increasing the relative humidity produced significant changes in the electrical resistance (R) of the PANI, indicating strong humidity-dependent characteristics similar to conventional CPs. In contrast, in the case of *in-situ* I₂ doping, the R and sensitivity of the PANI remained essentially unchanged when increasing the relative humidity, except for a very low sensitivity of 0.5% under 94% relative humidity. In addition, the R for the PANI with *in-situ* I₂ doping showed no aging effect, while the R for the *ex-situ*-doped PANI increased dramatically over time. Thus, it is anticipated that the use of *in-situ* doping during plasma polymerization can be widely used to design stable and high-performance CPs with humidity-independent characteristics for a variety of applications. *Published by AIP Publishing.* [<http://dx.doi.org/10.1063/1.4974222>]

The last fifty years have witnessed many significant advances and changes in the synthesis and characterization of conducting polymers (CPs).^{1–3} Conventionally, CPs have been synthesized via chemical, electrochemical, or photo-induced polymerization.^{1,4–7} However, plasma polymerization using atmospheric pressure plasma (APP) has recently been established as a simple and important method for synthesizing CPs.^{8–13} As previously reported, since the chemical structures of APP-polymerized CPs can be controlled by the plasma conditions,^{13–16} the characterization of the resulting CPs includes good adherence, high quality, pinhole-free, low resistance, and high crosslinking via dry and low temperature processes.^{8–13} Among CPs, polyaniline (PANI) has attracted particular interest due to its good electrical conductivity, low cost, and good environmental stability.^{2,17} PANI is also unique among the electrical CPs as its electrical properties can be reversibly controlled by changing the oxidation state of the main chain and via the protonation of the amine nitrogen chain.^{2,18–21}

While the structures and humidity dependence of chemically, photo-, or electrochemically synthesized PANI with a proton donor such as HCl and iodine (I₂) have already been extensively reported,^{22–25} the structures and humidity dependence of APP-polymerized PANI remain unclear. Most previous studies have focused on the electrical conductivity, chemical structure, and morphology of APP-polymerized PANI thin films with *ex-situ* HCl or I₂ doping.^{26–29} However,

more importantly, the conductivity of conventional CPs is significantly affected by the ambient humidity, which restricts their application, for example, in flexible display technologies and gas sensors.^{25,29–31} Therefore, it is important to synthesize the high-density CPs with humidity-independent properties as conductive layers for future display technologies, gas sensors, molecular electronics, optoelectronics, and bio-nanotechnology applications. Until now, there has been no report on a conductive polymer synthesized using APP polymerization techniques at room-temperature that is independent of the ambient humidity.

The current authors recently reported on an APP method for the synthesis of CPs, where the resulting plasma-polymerized PANI and polypyrrole (PPy) nanofibers showed high molecular weights and single-crystalline characteristics.^{8,9} Accordingly, this letter introduces the synthesis of high-density PANI thin films with humidity-independent conductivity via an advanced APP polymerization technique using *in-situ* I₂ doping at room-temperature. In particular, the variation in resistance of the *ex-situ* or *in-situ* I₂-doped PANI is examined under various humidity conditions and ambient air to check the suitability of the conductive layers for applications in future display and gas sensor technologies. The experimental results confirmed that PANI thin films with humidity-independent conductivity were obtained when using intense and broad APP polymerization with *in-situ* I₂ doping. The APP polymerization device employed in this research is described in detail in Ref. 8, except for the I₂ doping method. In this study, for the *ex-situ* I₂ doping, the PANI film samples were placed in a sealed container

^{a)}C.-S. Park and D. Y. Kim contributed equally to this work.

^{b)}Author to whom correspondence should be addressed. Electronic mail: hstae@ee.knu.ac.kr.

containing solid I_2 (1 g) after the deposition process, whereas for the *in-situ* I_2 doping, solid I_2 was vaporized by argon (Ar) gas at a flow rate of 16 standard cubic centimeters per minute (sccm) during the deposition process and vaporization of the aniline monomer solution.

As shown in Fig. 1(a), the conventional APP polymerization device also included a cylindrical plastic tube and an insulating substrate holder to minimize the quenching from the ambient air and increase the plasma energy and density in the nucleation region.⁸ However, in the case of the *in-situ* I_2 doping with advanced APP polymerization, more intense and stronger plasma was produced throughout the nucleation region, even though the applied voltages and total current were the same as those for the *ex-situ* I_2 doping, as shown in Fig. 1(b). This inferred that the advanced APP polymerization device using *in-situ* I_2 doping played an important role in minimizing the impurities for producing intense plasma as the vaporized active iodine easily absorbed various positive carriers, such as N_2^+ , N_2H^+ , H_2O^+ , H_3O^+ , O_2^+ , and

$O^+(H_2O)$, from the ambient air,³² resulting in an Ar-dominant gas condition in the nucleation region shielding the plasma generation region. In addition, in the case of the *in-situ* I_2 doping with advanced APP polymerization, the color of the plasma was brighter in the nucleation region, indicating that the vaporized iodine participated in the polymerization process. Figure 1(c) shows the emission spectra intensities measured in the nucleation region for analyzing the intensity of the reactive nitrogen, oxygen (OH radicals), Ar, and carbonaceous species, which then allowed the plasma energy state to be estimated using an optical emission spectrometer (OES). As shown in Fig. 1(c), in the case of *in-situ* I_2 doping, the intensity of the OH radical (308 nm) peak was significantly increased in the nucleation region during the nucleation process of the aniline monomer due to the absorption of H_2O^+ , H_3O^+ , O_2^+ , and $O^+(H_2O)$ in the ambient air via the active iodine. This means that the plasma state and fragmentation of the aniline monomer was affected by the *in-situ* I_2 doping during the APP polymerization.

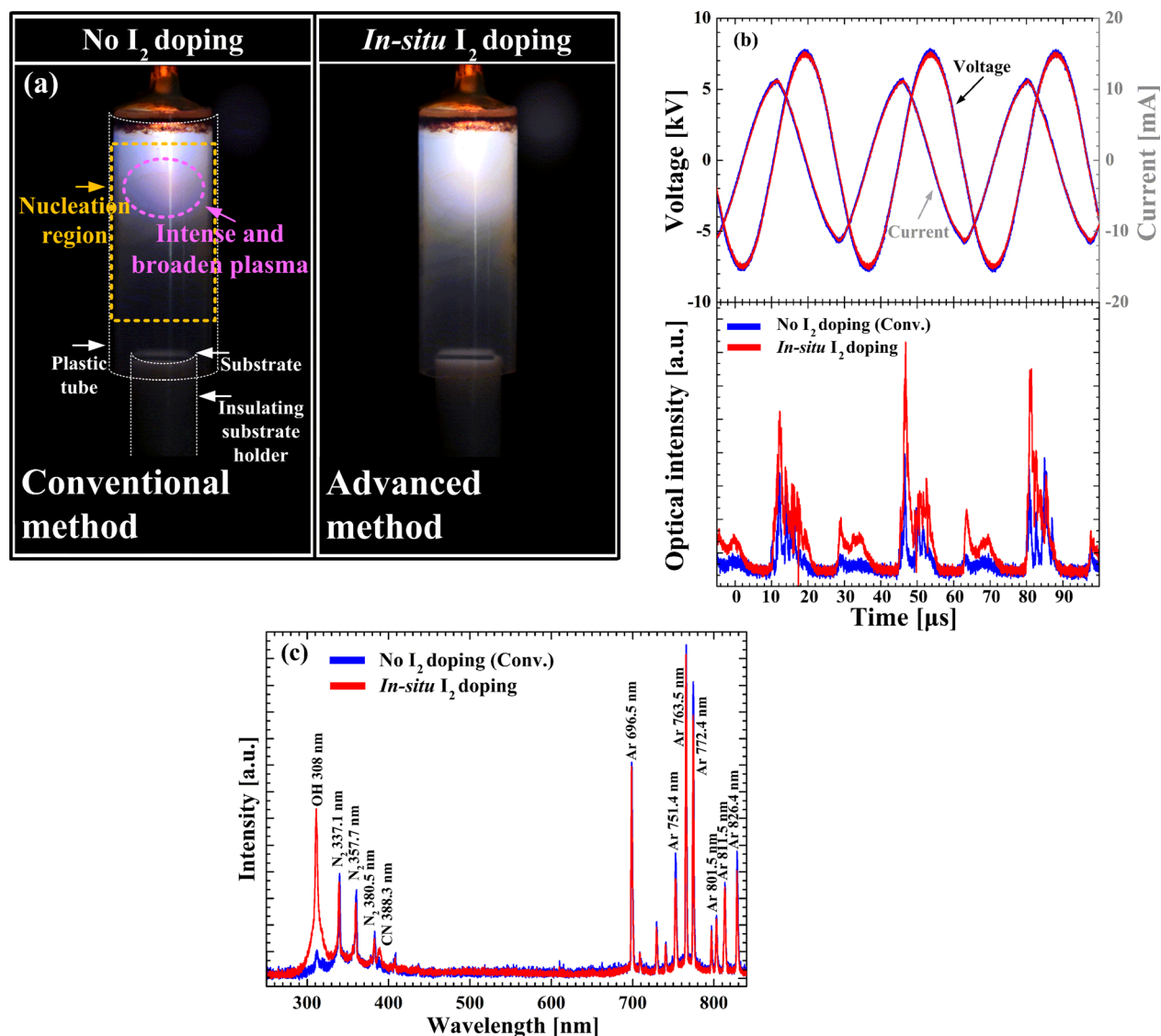


FIG. 1. (a) Images of plasma, (b) applied voltage, total current, and optical intensity, and (c) emission spectra intensities measured using optical emission spectrometer (OES) in nucleation region when applying advanced atmospheric pressure plasma (APP) polymerization device with no iodine (Conv.) and with *in-situ* iodine (I_2) doping technique.

The lack of any I₂-related peaks in the OES data with the *in-situ* I₂ doping can be attributed to the low I₂ dose in the plasma nucleation region.

Figure 2 shows the Fourier transform infrared spectroscopy (FTIR) spectra from the PANI thin films synthesized by the APP device using the *ex-situ* and *in-situ* I₂ doping techniques. As shown, the undoped PANI films exhibited an insulated state with an emeraldine base structure, were partially oxidized, and had a few N-H groups in the main chain.⁸ An emeraldine base structure can be changed to an emeraldine salt with electrical conducting characteristics by removing an electron from the N-H group using an I₂ doping technique. In the case of the *ex-situ* I₂ doping, most of the spectra peaks were significantly diminished and became smooth, presumably due to the absorption of hydrogen in the PANI films via the iodine. However, in the case of the *in-situ* I₂ doping, the peak intensities were significantly increased at 3210 cm⁻¹ (N-H stretching), 1652 cm⁻¹ (deformation structure), and 1430 cm⁻¹ (C-C stretching vibration), plus the sharp peaks at 891 cm⁻¹ and 758 cm⁻¹ were more intense in the *in-situ* I₂-doped plasma-polymerized PANI. These peaks have been assigned to the absorption of 1,4 disubstitution in the benzene ring and related to a better electrical conductivity.^{23,29,33} Therefore, the PANI synthesized by the advanced APP polymerization method using the *in-situ* I₂ doping technique apparently had a better electrical conductivity.

Figure 3 shows the scanning electron microscopy (SEM) images with the molecular weight (M_w) of the undoped and I₂-doped PANI thin films. The undoped PANI films consisted of nanoparticles and nanofibers with irregularly low cross-linked and highly porous networks. The diameters of the nanoparticles and nanofibers were about 8–10 nm and 10–20 nm, respectively.⁸ After the *ex-situ* doping, all the nanoparticles vanished and aggregation was observed between adjacent nanofibers. However, in the case of the *in-situ* I₂ doping, the morphology of the PANI was unaffected by the I₂ doping. Noticeably, despite the same deposition time, much denser polymer networks were obtained using the *in-situ* I₂ doping method when compared to the undoped PANI. Moreover, as

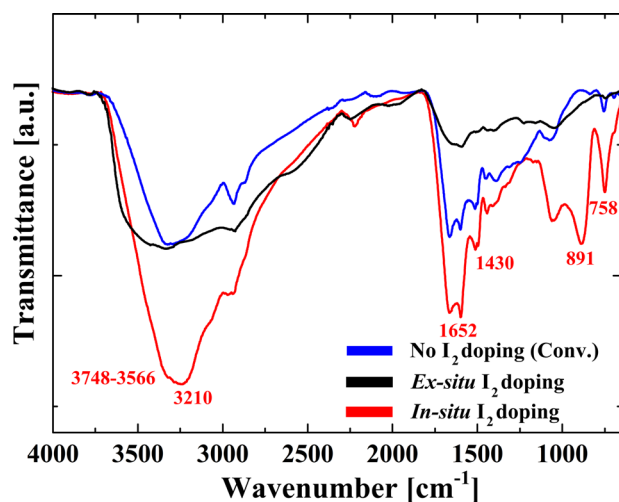


FIG. 2. Fourier transform infrared spectroscopy (FTIR) spectra of plasma-polymerized PANI thin films prepared using advanced APP polymerization device after 60-min deposition with no iodine, with 10-min *ex-situ* iodine doping after deposition, and with *in-situ* iodine doping during deposition.

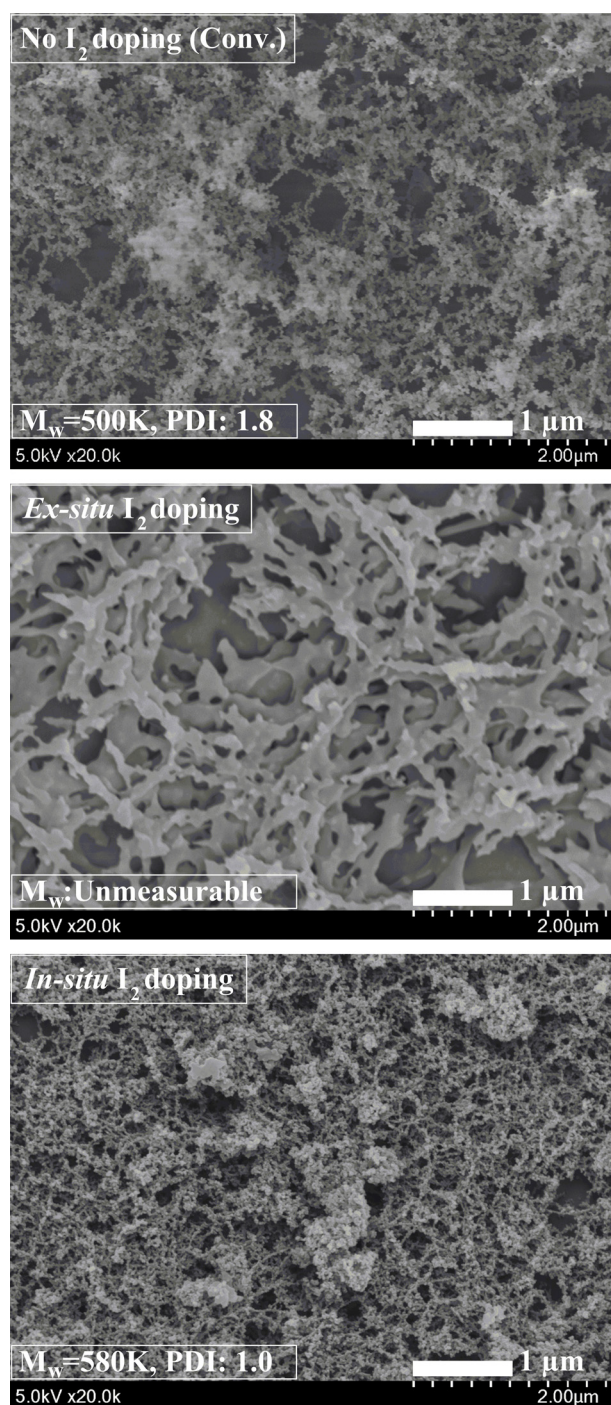


FIG. 3. Scanning electron microscopy (SEM) images with a molecular weight of plasma-polymerized PANI thin films prepared using advanced APP polymerization device after 20-min deposition with no iodine, with 5-min *ex-situ* iodine doping after deposition, and with *in-situ* iodine doping during deposition. Scale bar = 1 μm.

shown in Fig. 3, gel permeation chromatography revealed that the *in-situ* I₂-doped PANI thin films were of high quality with a high M_w of about 580 kDa and an excellent polydispersity index (PDI) of about 1.0. Thus, it is anticipated that the highly porous and nanofibrous networks in the *in-situ* I₂-doped PANI thin films can provide a unique advantage as active layers for application in gas sensors.

Figure 4(a) shows the changes in the surface resistance (R) of the plasma-polymerized PANI thin films in relation to the exposure time under ambient air. To measure the

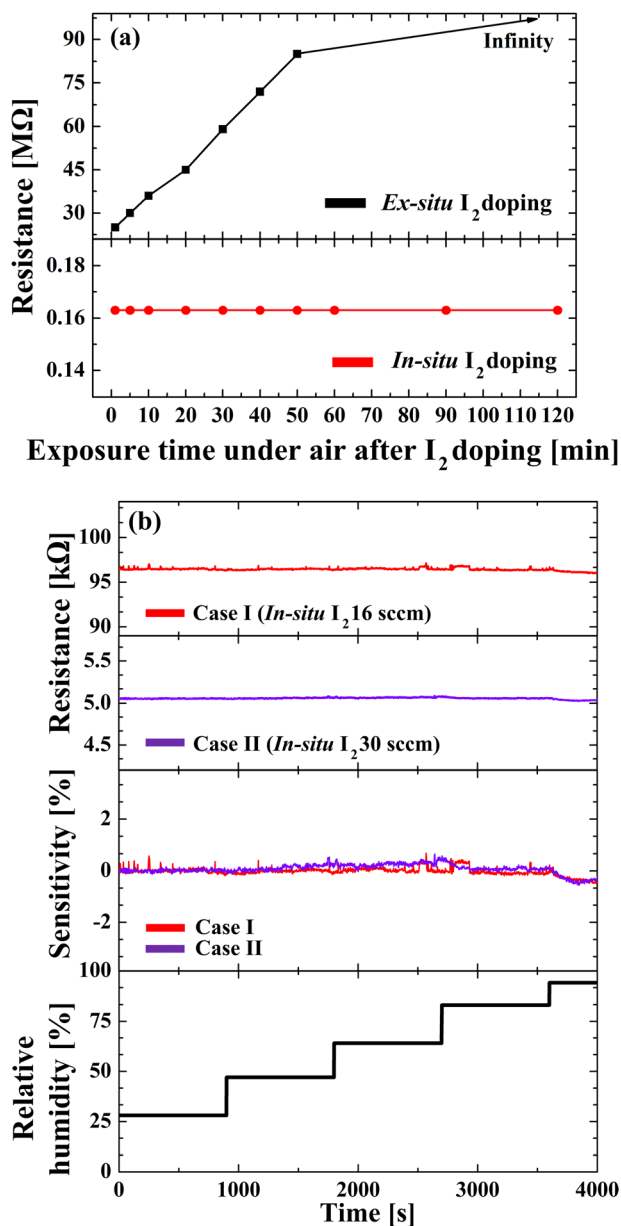


FIG. 4. (a) Changes in the resistance of plasma-polymerized PANI thin films: plasma-polymerized samples were treated with 5-min *ex-situ* iodine doping after deposition and *in-situ* iodine doping and then exposed to ambient air for various periods of time. (b) Variation of resistance and sensitivity with change in relative humidity (%) at an ambient temperature of 25 °C prepared using advanced APP polymerization device after 30-min deposition using *in-situ* iodine doping technique during deposition. Cases I and II used 16 and 30 sccm Ar gas flow rates for vaporizing iodine, respectively.

electrical resistance, the PANI thin films were synthesized on substrates supplied with interdigitated Pt electrodes. The *ex-situ* I₂ doping was conducted for 5 min right after the deposition of the PANI thin films. The initial R of the undoped PANI thin films was over $2 \times 10^9 \Omega$ (limit of instrument used). For the case of *ex-situ* I₂ doping, the initial R was still very high with a value of about $2.5 \times 10^7 \Omega$. However, this significantly decreased to about $1.6 \times 10^5 \Omega$ when using the *in-situ* I₂ doping method with the advanced APP polymerization technique. This may have been related to the very dense PANI networks composed of nanoparticles and nanofibers, as shown in Fig. 3. In the case of the *ex-situ* I₂ doping, when increasing the exposure time, the R linearly

increased and finally reached the measurement limit of $2 \times 10^9 \Omega$ after 50 min due to diffusion of the absorbed iodine out of the films.²⁹ Conversely, in the case of the *in-situ* I₂ doping, the R barely changed and only increased from 1.6×10^5 to $1.9 \times 10^5 \Omega$, even after 2 days of exposure to ambient air. This was because, in the case of the *in-situ* I₂ doping method, iodine (I₂), iodide (I⁻), and polyiodides (I₃⁻ and I₅⁻) could directly participate in the formation of charge transfer complexes during the plasma polymerization, allowing them to be homogeneously distributed throughout the PANI networks. Thus, the advanced APP polymerization using the *in-situ* method facilitated the efficient and continuous provision of charge carriers in the conductive PANI films without any diffusion of the absorbed iodine from the films. Consequently, the resistance of the plasma-synthesized PANI using the advanced APP jets with the *in-situ* I₂ doping technique was much more stable under ambient conditions than the *ex-situ* I₂-doped PANI.

Figure 4(b) shows the variation of the R and sensitivity^{34,35} of the *in-situ* I₂-doped PANI thin films as a function of the relative humidity, where cases I and II correspond to Ar gas flow rates of 16 and 30 sccm for the vaporising iodine, respectively. As shown in Fig. 4(b), the initial R was easily controlled using the flow rate of the carrier gas. In the case of the *ex-situ* I₂ doping, when increasing the relative humidity, the R changed significantly and showed strong humidity-dependent characteristics, similar to conventional polymer thin films [not shown here]. In contrast, with the *in-situ* I₂ doping, the R and sensitivity remained essentially unchanged when increasing the relative humidity, except for a sensitivity of 0.5% under 94% relative humidity, meaning that the PANI thin films synthesized using the advanced APP polymerization with *in-situ* doping exhibited humidity-independent characteristics. While a complete understanding of the independent characteristics of the electrical R under ambient air or different humidity conditions could not be reached and requires further study, it was still attributed to the difference in the doping process between *ex-situ* and *in-situ* doping. It is already known that the residual radicals in polymer networks can be oxidized in ambient air. That is, the reaction with iodine and the polymer oxidation process is competitive. Therefore, in the case of the *ex-situ* doping, some of the residual radicals in the polymer networks that formed C-I bonds upon *ex-situ* I₂ doping may have reacted with the atmospheric oxygen, thereby varying the electrical R depending on the ambient conditions. In contrast, in the case of the *in-situ* doping, the doping and polymerization processes occurred at the same time and formed homogeneous charge transfer complexes throughout the polymer networks, thereby reducing the possibility of oxidation upon exposure to the ambient air after polymerization. While oxidation inevitably occurred during the *in-situ* doping, it is supposed that the oxidation was also minimized due to the presence of the plastic tube and downward Ar flow of the plasma jet, which effectively blocked the introduction of oxygen from the ambient air.

In summary, the humidity-independence of the plasma-synthesized PANI thin films using advanced APP polymerization combined with an *in-situ* method was presumably related to the simultaneous formation of charge transfer

complexes during the nucleation of the monomer. The resistance remained stable under ambient air and various humidity conditions. Thus, it is anticipated that plasma-polymerized PANI thin films synthesized using the proposed advanced APP polymerization system can help to overcome the limitations of conventional polymerization systems. Furthermore, such PANI thin films with humidity-independent characteristics can provide a unique advantage as conductive layers for future gas sensors, display technologies, plasma thrusters, molecular electronics, optoelectronics, and bio-nanotechnology applications.

This research was supported by the National Research Foundation of Korea (NRF) grant funded by the Korea government (MSIP) (No. 2016R1C1B1011918).

- ¹D. N. Nguyen and H. Yoon, *Polymers* **8**, 118 (2016).
- ²M. S. Zoromba, N. A. El-Ghamaz, A. Z. El-Sonbati, A. A. El-Bindary, M. A. Diab, and O. El-Shahat, *Synth. React. Inorg., Met.-Org., Nano-Met. Chem.* **46**, 1179 (2016).
- ³H. Yoon, *Nanomaterials* **3**, 524 (2013).
- ⁴B. Narayanan, S. A. Deshmukh, L. K. Shrestha, K. Ariga, V. G. Pol, and S. K. R. S. Sankaranarayanan, *Appl. Phys. Lett.* **109**, 041901 (2016).
- ⁵S. Badhulika and A. Mulchandani, *Appl. Phys. Lett.* **107**, 093107 (2015).
- ⁶A. Abdolahi, E. Hamzah, Z. Ibrahim, and S. Hashim, *Materials* **5**, 1487 (2012).
- ⁷X. Meng, K. Fujita, Y. Zong, S. Murai, and K. Tanaka, *Appl. Phys. Lett.* **92**, 201112 (2008).
- ⁸C.-S. Park, D. H. Kim, B. J. Shin, and H.-S. Tae, *Materials* **9**, 39 (2016).
- ⁹C.-S. Park, D. H. Kim, B. J. Shin, D. Y. Kim, H.-K. Lee, and H.-S. Tae, *Materials* **9**, 812 (2016).
- ¹⁰M. Michel, J. Bour, J. Petersen, C. Arnoult, F. Ettingshausen, C. Roth, and D. Ruch, *Fuel Cells* **10**, 932 (2010).
- ¹¹K.-S. Chen, S.-C. Liao, S.-W. Lin, S.-H. Tsao, T. H. Ting, N. Inagaki, H.-M. Wu, and W.-Y. Chen, *Surf. Coat. Technol.* **231**, 408 (2013).
- ¹²H. R. Humud, M. M. Abdullah, and D. M. Khudhair, *Int. J. Curr. Eng. Technol.* **4**, 3405 (2014).
- ¹³K. Urabe, B. L. Sands, B. N. Ganguly, and O. Sakai, *Plasma Sources Sci. Technol.* **21**, 034004 (2012).
- ¹⁴J. Phillips, C. C. Luhrs, and M. Richard, *IEEE Trans. Plasma Sci.* **37**, 726 (2009).
- ¹⁵U. S. Sajeeb, C. J. Mathai, S. Sarvanan, R. R. Ashokan, S. Venkatachalam, and M. R. Anantharaman, *Bull. Mater. Sci.* **29**, 159 (2006).
- ¹⁶S. Ameen, M. Song, D.-G. Kim, Y.-B. Im, H.-K. Seo, Y. S. Kim, and H.-S. Shin, *Macromol. Res.* **20**, 30 (2012).
- ¹⁷M. Trchova and J. Stejskal, *Pure Appl. Chem.* **83**, 1803 (2011).
- ¹⁸N. V. Bhat and N. V. Joshi, *Plasma Chem. Plasma Process.* **14**, 151 (1994).
- ¹⁹J. Morales, M. G. Olayo, G. J. Cruz, M. M. Castillo-Ortega, and R. Olayo, *J. Polym. Sci., Part B: Polym. Phys.* **38**, 3247 (2000).
- ²⁰M. G. Olayo, J. Morales, G. J. Cruz, R. Olayo, E. Ordonez, and S. R. Barocio, *J. Polym. Sci., Part B: Polym. Phys.* **39**, 175 (2001).
- ²¹J. Morales, M. G. Olayo, G. J. Cruz, and R. Olayo, *J. Polym. Sci., Part B: Polym. Phys.* **40**, 1850 (2002).
- ²²S. Jain, S. Chakane, A. B. Samui, V. N. Krishnamurthy, and S. V. Boraskar, *Sens. Actuators* **96**, 124 (2003).
- ²³G. J. Cruz, J. Morales, M. M. Castillo-Ortega, and R. Olayo, *Synth. Met.* **88**, 213 (1997).
- ²⁴G. J. Cruz, M. G. Olayo, O. G. Lopez, L. M. Gomez, J. Morales, and R. Olayo, *Polymer* **51**, 4314 (2010).
- ²⁵G. J. Cruz, J. Morales, and R. Olayo, *Thin Solid Films* **342**, 119 (1999).
- ²⁶C. J. Mathai, S. Saravanan, M. R. Anantharaman, S. Venkatachalam, and S. Jayalekshmi, *J. Phys. D: Appl. Phys.* **35**, 2206 (2002).
- ²⁷M. Vasquez, G. J. Cruz, M. G. Olayo, T. Timoshina, J. Morales, and R. Olayo, *Polymer* **47**, 7864 (2006).
- ²⁸K. Hosono, I. Matsubara, N. Murayama, W. Shin, N. Izu, and S. Kanzaki, *Thin Solid Films* **441**, 72 (2003).
- ²⁹J. Wang, K. G. Neoh, and E. T. Kang, *Thin Solid Films* **446**, 205 (2004).
- ³⁰Y. Liu, S. Yao, Q. Yang, P. Sun, Y. Gao, X. Liang, F. Liu, and G. Lu, *RSC Adv.* **5**, 52252 (2015).
- ³¹J.-W. Yoon, J.-S. Kim, T.-H. Kim, Y. J. Hong, Y. C. Kang, and J.-H. Lee, *Small* **12**, 4229 (2016).
- ³²T. Ito, K. Gotoh, K. Sekimoto, and S. Hamaguchi, *Plasma Med.* **5**, 283 (2015).
- ³³M. Totolin and M. Grigoraş, *Rev. Roum. Chim.* **52**, 999 (2007).
- ³⁴A. M. Dumitrescu, G. Lisa, A. R. Iordan, F. Tudorache, I. Petrila, A. I. Borhan, M. N. Palamaru, C. Mihailescu, L. Leontie, and C. Munteanu, *Mater. Chem. Phys.* **156**, 170 (2015).
- ³⁵M. Parthibavarman, V. Hariharan, and C. Sekar, *Mater. Sci. Eng. C* **31**, 840 (2011).